Modelling and analysis of PV integrated ultra-high gain dc-dc converter for BLDC motor drives

Design, simulation, and performance evaluation for efficient electric vehicle applications.

[1]J. Swetha, [2]Dr. G. Jhansi Rani

[1]PG Student, [2]Assistant Professor

[1]Department of Electrical and Electronics Engineering,

[1]University College of Engineering, Osmania University, Hyderabad, India

[1]jatothswetha17@gmail.com, [2]jhansirani99@yahoo.co.in

***Abstract*— This study is about creating a system that uses solar power (PV) to run a Brushless DC (BLDC) motor, which is useful for things like electric vehicles and off-grid power. Because solar panels give a low and unstable voltage, we use a special switched-capacitor quadratic boost DC-DC converter to step it up to a much higher, steady voltage for the motor drive, while also keeping the power flow smooth. We use a control loop with a PI controller to keep this main DC voltage stable, and then this stable power goes to an inverter that uses sensor feedback from the motor to run the BLDC efficiently. Our simulation tests showed that even without the usual maximum power tracking (MPPT) system, the control setup successfully held the voltage steady, making the motor's speed and torque reliable; this confirms that our proposed converter design is a very efficient and suitable way to use solar energy for high-performance motor drives.**

***Index Terms*—Photo Voltaic (PV), BLDC motor, switched-capacitor quadratic boost DC-DC converter, PI controller, inverter, voltage, efficiency.**

I. INTRODUCTION

The global commitment towards sustainable energy makes the integration of Photovoltaic (PV) systems with technologies like Electric Vehicles (EVs) a vital area of research. While PV arrays offer clean power, their output is characterized by a low and highly fluctuating DC voltage, which poses a significant challenge for directly powering high-performance loads like motor drives. This situation mandates the use of an efficient power electronic converter to precisely raise the voltage to the required level. Brushless DC (BLDC) motors are widely adopted for EV applications due to their high efficiency and low maintenance demands. However, standard boost converters often struggle to deliver the high voltage gain necessary to bridge the gap between the low PV output and the motor drive's requirement, frequently leading to poor efficiency and high component stress. To address this, this paper proposes the design and simulation of a PV-fed BLDC motor drive system that utilizes an advanced switched-capacitor quadratic boost converter. This novel topology is selected for its ability to achieve ultra-high voltage gain at a moderate operating condition, which significantly reduces voltage stress and input current ripple. Through a rigorous analysis of the system's performance under various sunlight and load changes in simulation, this research aims to provide a reliable solution for developing highly efficient and robust renewable energy-powered drive systems.

II. SYSTEM MODELLING AND DESIGN

The complete proposed system integrates three main sub-systems: the Photovoltaic (PV) array as the source, the Switched-Capacitor Quadratic Boost Converter (SCQBC) for high-gain power conversion, and the Brushless DC (BLDC) motor drive. A precise mathematical model for each component is essential for accurate simulation and performance analysis in MATLAB/Simulink.

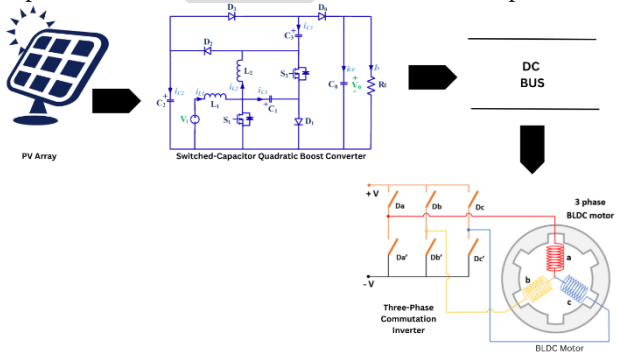

Figure 1. Block diagram of Proposed System.

A. Photovoltaic (PV) Array Model

The PV array serves as the primary energy source. Its performance is highly dependent on ambient temperature and solar irradiance. For simulation accuracy, the PV panel is modelled using the widely accepted single-diode model. This model mathematically captures the non-linear Current-Voltage (I-V) characteristics of a solar cell, which is crucial for accurately representing the system's input under varying sunlight. The output current (I_{PV}) is calculated based on the generated photocurrent (I_{ph}), diode saturation current (I_o), and parameters like series resistance (R_S) and shunt resistance (R_{sh}). The key equations establish the relationship between the cell current, cell voltage, and environmental factors, ensuring that the model accurately reflects real-world PV behaviour.

Table 1 PV ARRAY CONFIGURATION

Parameter	Module Value	Array value
Open-circuit voltage V_{oc} (V)	14.5	29.00
Short-circuit current I_{sc} (A)	5.5	55.00
Voltage at MPP V_{mp} (V)	11.9	23.80
Current at MPP I_{mp} (A)	5.3	53.00
Max Power I_{max} (W)	63.07	1261.40

B. Switched-Capacitor Quadratic Boost Converter

To bridge the significant voltage gap between the low PV output and the high DC bus required by the BLDC motor, the SCQBC is employed. This converter topology is chosen over conventional boost converters because it provides an ultra-high voltage gain at a manageable duty cycle (D), preventing the extreme switching conditions that cause high stress and loss in standard converters. The SCQBC achieves this gain by combining a traditional boost stage with a voltage multiplier cell based on switched-capacitor techniques.

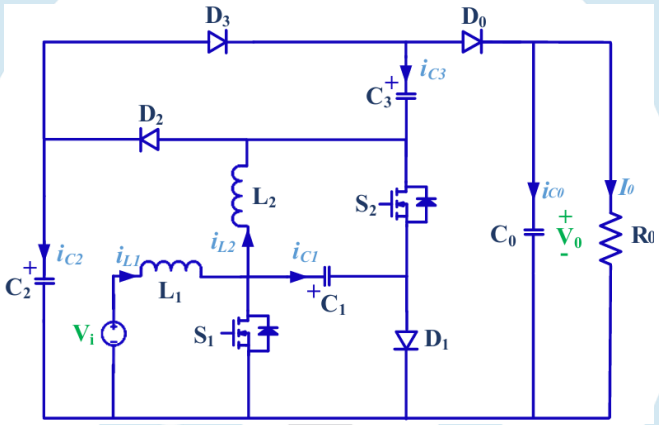

Figure 2. Schematic of the switched-capacitor quadratic boost converter.

The theoretical voltage gain (M) of the SCQBC is given by the following relationship.

$$M = \frac{V_{out}}{V_{in}} = \frac{1+D}{(1-D)^2} \qquad (1)$$

This quadratic relationship ensures a steep increase in output voltage (V_O) even when the duty cycle is moderate, which is a major advantage. The design involves careful selection of the inductor (C), input capacitor (C_{in}), and switched-capacitors (C_1, C_2) to minimize input current ripple and maintain efficiency under high voltage boost conditions.

1) Operating Principle and Mode Analysis

The converter operates in two main switching states within each switching period Ts, controlled by the duty cycle D of the switches.

- **Mode 1 (Switches ON):** Both switches S_1 and S_2 are turned ON simultaneously. During this interval, inductors L_1 and L_2 are connected to the input voltage source V_{in} and store energy while the capacitors discharge to maintain the load voltage.

$$V_{L1} = V_i \; ; \; V_{L2} = V_{C1} \qquad (2)$$

- **Mode 2 (Switches OFF):** Both switches turn OFF. Inductors L_1 and L_2 release stored energy via the diode-capacitor network, charging the capacitors and supplying energy to the load. When the gate pulse is withdrawn for the two switches at instant t_1, this mode of operation begins. The inductor L_1, along with the source V_i, charges capacitor C_1. With diode D_0 conducting, inductors L_1 and the source, along with capacitor C_3, power load R_0 and capacitor C_0. The inductor voltage profile is expressed as

$$V_{L1} = V_i - V_{C1}; \; V_{L2} = V_{C1} + V_{C3} - V_0 \qquad (3)$$

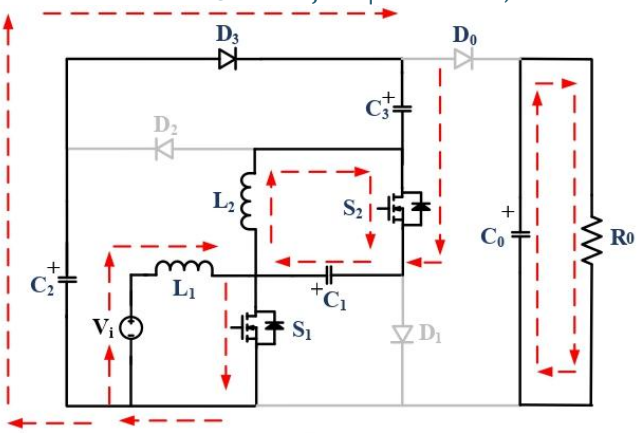

Figure 3. Operating of SCQBC converter in continuous conduction Mode 1.

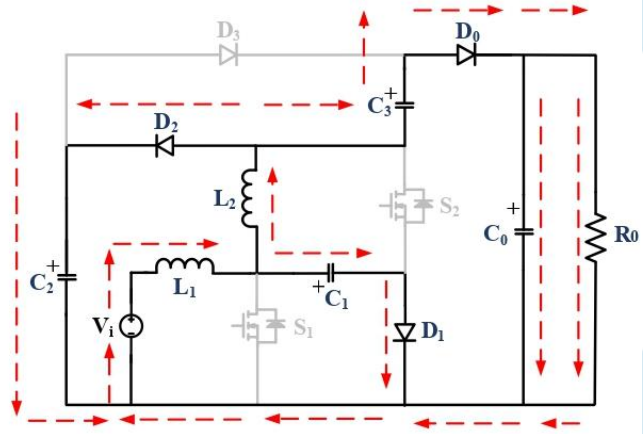

Figure 4. Operating of SCQBC converter in continuous conduction Mode 2.

C. BLDC Motor Drive System

Before the drive system consists of a three-phase voltage source inverter (VSI) and the BLDC motor itself. The VSI converts the regulated high DC bus voltage into the required trapezoidal-shaped voltages for the motor phases. The motor operates based on the principle of electronic commutation, where the switching of the VSI is directly governed by the rotor position feedback. Hall effect sensors, placed 120 degrees apart in the motor, provide signals indicating the rotor's precise position. This 6-step commutation process ensures the motor windings are energized sequentially, generating continuous torque. The dynamic model of the BLDC motor is described by its voltage equations and the mechanical equation, linking the electromagnetic torque (T_e) to the rotor speed (ω_r) and load torque (T_L):

$$V_{an} = R_a i_a + L_a \frac{di_a}{dt} + e_a \quad (4)$$

$$T_e = \frac{1}{\omega_m}(e_a i_a + e_b i_b + e_c i_c) \quad (5)$$

III. CONTROL STRATEGY

For the reliable operation of the Brushless DC (BLDC) motor drive, it is essential to maintain a stable and regulated voltage on the DC bus, which feeds the motor inverter. This section details the closed-loop control strategy employed for the Switched-Capacitor Quadratic Boost Converter (SCQBC) to achieve this regulation.

A. DC Bus Voltage Regulation

The primary control objective is to ensure that the output voltage of the SCQBC (V_{DC}) remains constant at its desired reference value (V_{Ref}), irrespective of changes in the input (solar irradiance) or output load (motor torque). This system operates by using a feedback mechanism, as shown in the control block diagram. The control loop is executed as follows:

1) **Sensing:** The actual DC bus voltage (V_{DC}) is measured continuously.

2) **Error Calculation:** This measured voltage is subtracted from the predefined reference voltage (V_{Ref}), generating an error signal (E).

3) **Controller Action:** This error signal is then fed into a Proportional-Integral (PI) controller.

The PI controller is the core of the voltage regulation system. It calculates the necessary corrective action by combining two terms: the Proportional term, which reacts to the current magnitude of the error, and the Integral term, which eliminates steady-state errors over time. This dual action is vital for robust performance under dynamic conditions.

B. Duty Cycle Generation

The control signal (u) generated by the PI controller represents the required duty cycle (D) needed by the SCQBC switch to either increase or decrease the output voltage. This signal is compared against a high-frequency sawtooth or triangular carrier wave using a Pulse Width Modulation (PWM) technique. The output of this comparison is the final switching pulse (G) that drives the main power switch of the SCQBC. By continuously adjusting the duty cycle based on the error signal, the SCQBC effectively regulates the DC bus voltage, providing a stable source for the motor.

C. Motor Commutation Strategy

The second part of the control system is dedicated to running the BLDC motor efficiently. Since the BLDC motor operation requires precise synchronization between the stator winding excitation and the rotor position, a six-step electronic commutation technique is used. Hall effect sensors fixed on the stator provide six distinct signals corresponding to the rotor position in 60°. These signals are used to generate the appropriate switching sequence for the three-phase inverter, ensuring that only two out of the three motor phases are energized at any given time to produce maximum torque. This sensor-based commutation strategy ensures reliable start-up and smooth running of the motor.

IV. SIMULATION AND RESULTS

The simulation of the proposed PV-fed BLDC motor drive system is performed using MATLAB/Simulink, a widely adopted platform for Modelling, simulation, and control design of power electronics and electric drives. Simulink's specialized toolboxes like Simscape Electrical allow detailed Modelling of electrical components, power converters, and control systems. The visual block-diagram approach enables flexible system integration and real-time dynamic analysis. The models incorporate standard PV array blocks, switched-capacitor DC-DC converter components, inverter circuits, and BLDC motor dynamics alongside closed-loop control algorithms.

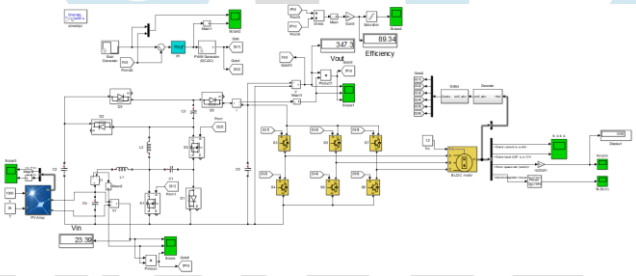

Figure 5. Simulation block of PV-fed BLDC under dynamic conditions.

Figure 5 depicts the simulation block diagram of the PV-fed BLDC motor system operating under dynamic conditions. This comprehensive simulation model integrates multiple subsystems to accurately represent real-world operation. It includes the photovoltaic array model, which captures the nonlinear and irradiance-dependent behaviour of the PV source. A switched-capacitor quadratic boost converter (SCQBC) interface follows, designed to boost the variable PV voltage to a regulated DC link voltage suitable for motor operation. The block further incorporates the BLDC motor model with electronic commutation control based on rotor position feedback, enabling the generation of phase currents and back EMF under varying load and speed conditions.

Figure 6 shows the rotor speed of the BLDC motor under different voltages during dynamic conditions. The motor speed initially rises rapidly from zero, reaching approximately 2900 rpm at 0.1 seconds, demonstrating strong acceleration as supply voltage increases. Around 0.2 seconds, the speed further increases to about 4000 rpm, indicating a higher voltage input or power availability. At about 0.5 seconds, the rotor speed drops sharply to nearly 2500 rpm, reflecting a voltage reduction or load increase, before rising back to about 3400 rpm at 0.8 seconds. This waveform reflects the motor's quick and stable response to varying voltage inputs, essential for effective operation in systems with fluctuating supply like PV-fed drives. The speed transitions occur smoothly without excessive oscillations, showing good control robustness and torque management during transient and steady-state phases.

Table 2 Key parameters used in the simulation

Parameter	Value
PV Array Voltage (nominal)	$20V$
Output DC Bus Voltage	$400V$
Power Rating (W)	$250W$
Switching Frequency (f_s)	$20kHz$
Inductors L_1 and L_2	$130\mu H, 700\mu H$
Capacitors C_0, C_1, C_2, C_4	$83\mu F, 25\mu F, 27\mu F, 21\mu F$
Motor Rated Speed	$4000rpm$
Motor Rated Torque	As per load
Ambient Temperature Range	25°C (nominal)

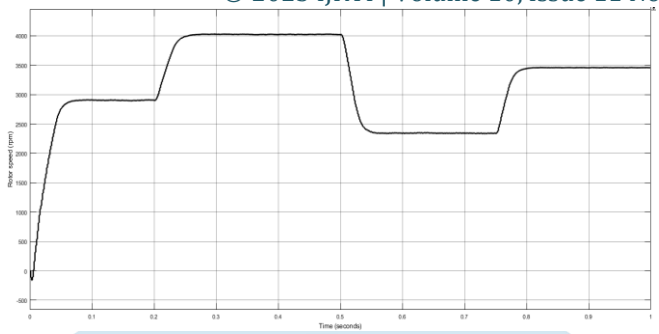

Figure 6 Rotor Speed at Different Voltages under dynamic conditions.

Figure 7 shows the electromagnetic torque response of the BLDC motor under dynamic voltage conditions. At startup, the torque quickly rises to about 2.3 Nm and then stabilizes close to 1.3 Nm. Each change in input voltage (corresponding to earlier speed steps) results in a noticeable torque peak or dip: a spike to 1.7 Nm when voltage increases, and a deep drop to around 0.5 Nm when voltage is reduced. Following each transient, the torque returns to its steady-state value. The waveform demonstrates robust dynamic response, smooth recovery, and effective torque control during variable supply scenarios.

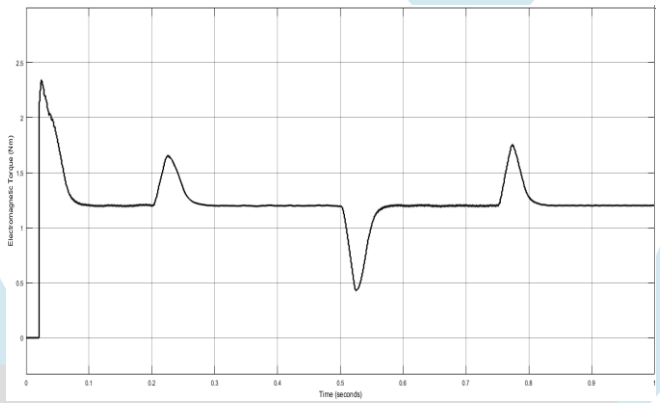

Figure 7 Torque at Different Voltages under dynamic conditions.

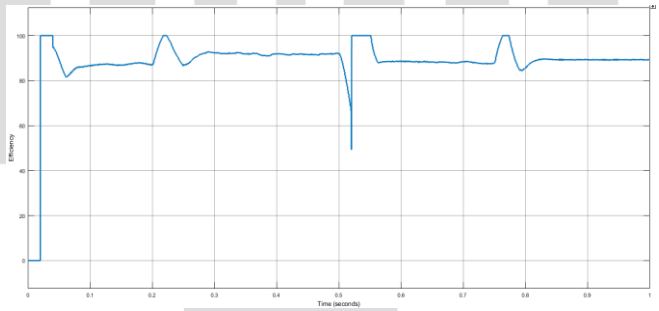

Figure 8 Efficiency at Different Voltages under dynamic conditions.

Figure 8 shows the efficiency of the BLDC system under dynamic voltage conditions. The efficiency initially rises quickly, reaching near 100%, then fluctuates between 85% and 95% during normal operation. Each change in input voltage results in a distinct efficiency peak or dip—a spike above 95% occurs when speed rises, and a sharp drop to nearly 50% is observed when voltage decreases abruptly. After each transition, the efficiency returns and stabilizes near its previous level. These variations highlight the system's quick adaptation and transient losses, demonstrating robust but dynamically sensitive performance under changing supply voltages.

In conclusion, this research validates a high-performance PV-powered BLDC motor drive system leveraging a novel switched-capacitor quadratic boost converter and three-phase inverter. The system's ability to maintain stable motor operation under fluctuating renewable input lays a solid foundation for further work on sustainable electric drive technologies, moving toward greener and more efficient energy usage in industrial and automotive applications.

REFERENCES

[1] L. Schmitz, D. C. Martins, and R. F. Coelho, "Generalized High Step-Up DC-DC Boost-Based Converter With Gain Cell," IEEE Trans. Circuits Syst. I, Regul. Pap., vol. 64, no. 2, pp. 480-493, Feb. 2017, doi: 10.1109/TCSI.2016.2603782.J. Clerk Maxwell, A Treatise on Electricity and Magnetism, 3rd ed., vol. 2. Oxford: Clarendon, 1892, pp.68–73.

[2] W. Li and X. He, "Review of Nonisolated High-Step-Up DC/DC Converters in Photovoltaic Grid-Connected Applications," IEEE Trans. Ind. Electron., vol. 58, no. 4, pp. 1239-1250, Apr. 2011, doi: 10.1109/TIE.2010.2049715.

[3] M. F. Baba, A. V. Giridhar, and B. L. Narasimharaju, "Nonisolated high gain hybrid switched-inductor DC-DC converter with common switch grounding," *Int. J. Circ. Theor. Appl.*, vol. 50, no. 8, pp. 2810-2828, 2022, doi: 10.1002/cta.3295.

[4] M.-K. Nguyen, T.-D. Duong, and Y.-C. Lim, "Switched-Capacitor-Based Dual-Switch High-Boost DC–DC Converter," *IEEE Trans. Power Electron.*, vol. 33, no. 5, pp. 4181-4189, May 2018, doi: 10.1109/TPEL.2017.2719040.

[5] S. Miao, W. Liu, and J. Gao, "Single-Inductor Boost Converter With Ultrahigh Step-Up Gain, Lower Switches Voltage Stress, Continuous Input Current, and Common Grounded Structure," *IEEE Trans. Power Electron.*, vol. 36, no. 7, pp. 7841-7852, Jul. 2021, doi: 10.1109/TPEL.2020.3047660.

[6] Y. Tang, D. Fu, T. Wang, and Z. Xu, "Hybrid Switched-Inductor Converters for High Step-Up Conversion," *IEEE Trans. Ind. Electron.*, vol. 62, no. 3, pp. 1480-1490, Mar. 2015, doi: 10.1109/TIE.2014.2364797.

[7] M. Samiullah et al., "High Gain Switched-Inductor-Double-Leg Converter With Wide Duty Range for DC Microgrid," IEEE Trans. Ind. Electron., vol. 68, no. 10, pp. 9561-9573, Oct. 2021, doi: 10.1109/TIE.2020.3028794.

[8] E. H. Ismail, M. A. Al-Saffar, A. J. Sabzali, and A. A. Fardoun, "A Family of Single-Switch PWM Converters With High Step-Up Conversion Ratio," IEEE Trans. Circuits Syst. I, Regul. Pap., vol. 55, no. 4, pp. 1159-1171, May 2008, doi: 10.1109/TCSI.2008.916427.

[9] R. Gules *et al.*, "A Modified SEPIC Converter With High Static Gain for Renewable Applications," *IEEE Trans. Power Electron.*, vol. 29, no. 11, pp. 5860-5871, Nov. 2014, doi: 10.1109/TPEL.2013.2296053.

[10] S. Saravanan and N. R. Babu, "Design and Development of Single Switch High Step-Up DC–DC Converter," IEEE J. Emerg. Sel. Topics Power Electron., vol. 6, no. 2, pp. 855-863, Jun. 2018, doi: 10.1109/JESTPE.2017.2739819.

[11] P. K. Maroti et al., "A New Structure of High Voltage Gain SEPIC Converter for Renewable Energy Applications," IEEE Access, vol. 7, pp. 89857-89868, 2019, doi: 10.1109/ACCESS.2019.2925564.

[12] T. S. Ambagahawaththa, D. Nayanasiri, A. Pasqual, and Y. Li, "A Design Methodology to Synthesize First Degree Single-Path Hybrid DC–DC Converters," IEEE Trans. Power Electron., vol. 37, no. 10, pp. 12336-12345, Oct. 2022, doi: 10.1109/TPEL.2022.3176201.

[13] V. Karthikeyan, S. Kumaravel, and G. Gurukumar, "High Step-Up Gain DC–DC Converter With Switched Capacitor and Regenerative Boost Configuration for Solar PV Applications," *IEEE Trans. Circuits Syst. II, Express Briefs*, vol. 66, no. 12, pp. 2022-2026, Dec. 2019, doi: 10.1109/TCSII.2019.2892144.

[14] G. G. Kumar, K. Sundaramoorthy, V. Karthikeyan, and E. Babaei, "Switched Capacitor–Inductor Network Based Ultra-Gain DC–DC Converter Using Single Switch," IEEE Trans. Ind. Electron., vol. 67, no. 12, pp. 10565-10574 (estimated from the DOI and typical page counts), Dec. 2020 (estimated from volume/number), doi: 10.1109/TIE.2019.2962406.

[15] G. R. Chandra, G. Pavani, A. Mounica, and Neetoori Radha Krishna, "Vidyut Dvichakrika - A hybrid electric bicycle," Australian Patent 2021106709, Aug. 24, 2022.